Data in brief 28 (2020) 104842

Contents lists available at ScienceDirect

Data in brief

journal homepage: www.elsevier.com/locate/dib

Data Article

Cytochrome *c* aggregation: A dataset at and far from the isoelectric point

Marilena Carbone [a, *], Alessandro Nucara [b], Marina Carbonaro [c]

[a] *Department of Chemical Science and Technologies, University of Rome Tor Vergata, Via della Ricerca Scientifica 1, 00133, Rome, Italy*
[b] *Department of Physics, Sapienza University of Rome, P.le A. Moro 5, 00185, Rome, Italy*
[c] *Council for Agricultural Research and Economics (CREA), Research Centre for Food and Nutrition, Via Ardeatina 546, 00178, Rome, Italy*

ARTICLE INFO

Article history:
Received 5 August 2019
Received in revised form 21 October 2019
Accepted 11 November 2019
Available online 18 November 2019

Keywords:
Protein fibrils
Particulates
Aggregates
Cytochrome *c*
SEM images
ThT fluorescence

ABSTRACT

We present SEM, ThT fluorescence and circular dichroism (CD) data of amyloidogenic aggregates of cytochrome *c* (cyt *c*).This protein is of outmost relevance in many biochemical processes, such as respiratory chain in mitochondria and cells apoptosis. The present data focus on polymorphism of the protein aggregates obtained at the isoelectric point (IP) and by changing the environmental pH above and below the IP, the protein concentration and the base. The SEM images provide evidence for a large variety of structures, depending on the pH and on protein concentration: mature amyloid fibrils and overstructured platelets are distinguishable in the aggregates below IP, and relatively high cyt *c* concentration, whereas inhomogeneous amyloid formations are observed above it. At pH 10, i.e. close to IP, only characteristic protein particulates at the micrometric scale are observed. SEM and Fluorescence data have been acquired in dried drops of protein solution, prepared in different bases: TRIS-HCl, at the different pH values, or NaOH (pH 13). Along with this, at relatively low cyt *c* concentration compact layered structures are visible below the IP, though still made of a thin fibrils reticulate, whereas above the IP, also at low cyt *c* concentration, granulates structures are present, merging into compact layer, alongside with platelets and mature fibers. These areas are characterized by diffuse ThT-fluorescence and typical fibrils. The loss of the predominant alpha helix

* Corresponding author.
E-mail addresses: carbone@uniroma2.it, marilena.carbone@roma2.infn.it (M. Carbone).

https://doi.org/10.1016/j.dib.2019.104842

secondary structure was verified by CD spectra. Besides the intrinsic scientific relevance, this data collection provides a set of images useful for spectroscopists to discriminate among different morphologic protein formations and suggests pathways for the achievement of different kinds of cytochrome *c* aggregates.
These data are add-ons of the paper published in the International Journal of Biomacromolecules, 138 (2019) 106–115, https://doi.org/10.1016/j.ijbiomac.2019.07.060.

Specifications Table

Subject	Biomolecules aggregation
Specific subject area	Cytochrome *c* aggregation: formation of amyloid fibrils and/or inhomogeneous aggregates at and close the protein isoelectric point
Type of data	Images Graph Table
How data were acquired	Zeiss Auriga Field Emission-Scanning Electron Microscope instrument operating at 7 kV. Zeiss optical microscope equipped with a mercury-vapor short-arc-lamp HB = 50 W/AC and 10 × objective in the emission spectral range centered at 525 ± 25 nm. Jasco J-1500 circular dichroism spectrophotometer, equipped with a thermostated cell holder set at 298 ± 0.5 K and purged with ultra-pure nitrogen gas.
Data format	Treated images in jpg format. Graph in xy form.
Parameters for data collection	Samples preparation: solutions of cytochrome *c* and TRIS-HCl, or NaOH at a variable ratios were prepared, the pH was adjusted close to the isoelectric point or at selected pHs and incubated at 70 °C. Aliquots of the sample were drawn out at regular intervals and repeatedly rinsed prior to SEM and ThT fluorescence imaging. SEM imaging: the rinsed samples were deposited on clean S (100) wafers, dried and placed on the microscope sample-holder. The imaging was performed in in-lens mode. ThT- Fluorescence: aliquots of the incubated samples were stained with ThT, rinsed with deionized water, deposited on microscope slides and dried in-air. CD-measurements: aliquots of the incubated samples were diluted in distilled water and poured in quarts cuvettes. CD spectra were taken in the far-UV range under ultrapure nitrogen flow, at room temperature.
Description of data collection	SEM: Scanning the images at different magnifications and rastering the whole silicon wafer surface to get a complete overview Fluorescence imaging: the collection of the data was carried out at different focal distances and magnifications.
Data source location	Department of Physics, Sapienza University, Rome, Italy Department of Chemical Science and Technologies, University Tor Vergata, Rome, Italy
Data accessibility	With this article

Value of the Data

- Cytochrome *c* aggregates morphology is rather changing, as the presence of molecular assemblies in the shape of platelets, spherules and fibers at micrometric scale has been detected and discussed in a number of studies. The route to aggregation of the protein depends on environmental pH, above and below the isoelectric point, and on protein concentration. The present data focus on a set of cytochrome *c* aggregates, obtained at and close to the isoelectric point, that can be useful as templates for amyloidogenic formations among the manifold of protein aggregates.
- SEM and Fluorescence data here reported represent a resource for biologists and life-science experts as well: indeed cytochrome *c* is a metalloprotein involved in both life and death (apoptosis) choice of cells, and it represents a model for both aggregation and fibrillation mechanisms in multi-functional heme enzymes. The property of cytochrome *c* to form superstructures with different morphologies by properly choosing concentration, base and incubation time, makes it appealing for its possible employment as a functional material: recently, creation of porous nanostructures for toxic gas sensing and use as catalytic agent to achieve high densities of metallo-porphyrins on the surface of an amyloid fibril have been advised.

- The present data may be used a basis for further investigation on amyloid aggregate of heme enzymes. The routes towards aggregation in these proteins strongly depend on the initial ionic strength of the solution and on the base/protein concentration, occurrences that produce a large number of topological aggregate types, each one with a different morphology and structure. Experiments aimed at studying amyloid fibrils of heme enzymes may take advantage of these data that would provide a prompt landmark.

Further insights in the study of heme protein aggregates will involve spectroscopic and microscopic experiment as well. In fact, even if the actual data provide an exhaustive phenomenological scenario, few is still known about the structure of cytochrome *c* molecules embedded in the aggregates. Therefore, spectromicroscopy investigation by advanced techniques might enlighten secondary and tertiary structures of the protein molecules in the different complexes.

- The completeness of this dataset ensures additional value to the whole implant, as they provide insight in the cyt *c* aggregation below, above and at the isoelectric point. Especially the latter is newly disclosed information, as no studies were reported so far on the aggregation of a low amyloidogenicity protein such as cyt *c* at the IP.

1. Data

Cyt *c* aggregation is highly versatile, with the possibility of directing the morphology towards different forms, depending on the environmental conditions. The panorama is quite motley and here we present data to expose the possible variants, focussing mostly on conditions to achieve compact structures and particulates. For comparison purposes, data are reported on the fibrillation in the high protein concentration regime below the IP, where it is known that a mixture of prefibrils, fibrils, mature fibers, and platelets are formed [1]. Compact cyct c morphologies made of granules are also obtained well above the IP and are subsequently reported. In Table 1 a summary is reported describing the cyt *c* aggregation conditions (protein concentration and pH), presented in this paper along with the associated structures.

The most striking feature is the cyt *c* aggregation at the IP, which is spelt out in Fig. 1a) and b) by SEM images. Roundish unstructured particulates are observed with relatively mono-disperse size in the micrometer range. Though the formation of such particulates was detected at the IP for a number of amyloid proteins, including bovine β-lactoglobulin, bovine serum albumin, bovine insulin, horse heart myoglobin, hen egg white lysozyme, equine lysozyme, human transthyretin, human α-synuclein and insulin, no observations were reported, so far, on a low amyloidogenicity protein such as cyt *c* with comparable morphology [2,3]. When deposited on the silicon sample-holder, the overall envelop of particulates can be characterized by of large number of units (i.e. roundish particulates) as in Fig. 1a) or of only a few ones as in Fig. 1b).

The scenario away from the IP can be quite complex as the aggregation was hypothesized to be driven by two simultaneous kinetic processes, a slow and a fast one [1], leading to an envelope of interconnected β-rich structures and less structured foils, in the forms of mature fibers, pre-fibrils and platelets. This typical scenario is epitomized in Fig. 2a) where the bundle of all aggregates arrangements are present. The fibril nature of the interconnected structures is verified by ThT fluorescence, as reported in Fig. 2b).

The protein concentration plays a key role in directing the prevalence of a structure over the others. The incubation of cyt *c* at a relatively low concentration (i.e. 92 μM) leads the aggregation towards compact layered assemblies, already after ½ hour incubation, as in Fig. 3a) where parallel or nearly parallel ripples are observed as highlighted by the yellow arrows. The internal structure can be appreciated in areas where sections of the layers are exposed. This is the case of the area highlighted by

Table 1
Summary of the cyt *c* aggregation conditions reported in this paper; Cp = protein concentration. In the most right column the morphology associated with each set of parameters is indicated. Regular stands for the mixture of pre-fibrils, fibrils, mature fibers, and platelet, typical in those experimental conditions.

Base	Cp	pH	Morphology
Tris-HCl	530 μM	~10, IP	Particulate
Tris-HCl	625 μM	9, Below IP	Regular
Tris-HCl	92 μM	9, Below IP	Compact
NaOH	100 μM	13, Above IP	Platelets + granulates

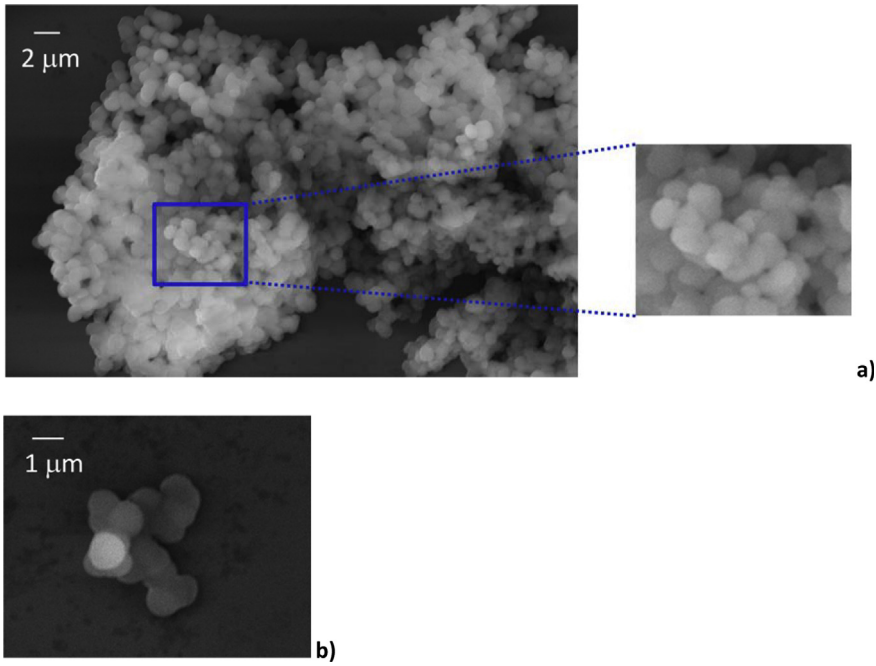

Fig. 1. SEM images of samples of cyt *c* aggregated via Tris-HCl at the isoelectric point after 5 h incubation.

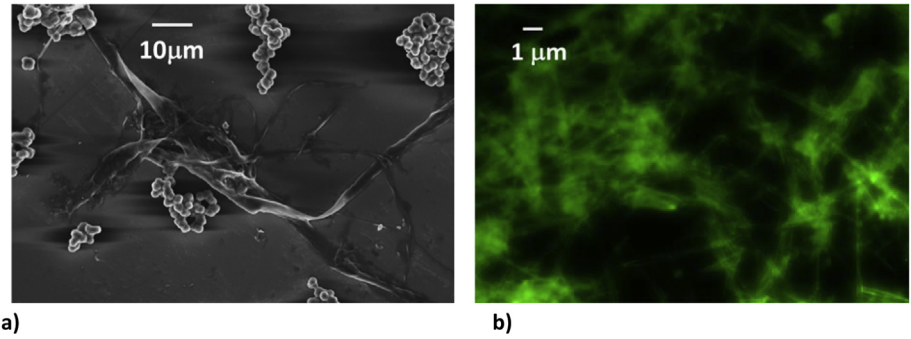

Fig. 2. a) SEM images of samples of cyt *c* aggregated via Tris-HCl below the IP, after 1 h incubation; b) fluorescence image of the same sample treated with ThT.

the green rectangle, which magnified in Fig. 3b). The inspection of this area reveals a mesh of thin elongated aggregates which run in all directions to form sort of nests.

The aggregation at a pH well above the IP causes a rapid hydrophobic collapse. The aggregation kinetic processes are still twofold, a fast and a slow one [1], but the tuning towards platelet fabrication is more efficient, to the limit of gaining again compact structures. After 1 hour incubation of cyt *c* at a relatively low concentration of protein, i.e. 100 μM, extended platelets are observed amidst thick granulate textures aggregates (Fig. 4). The interconnection between platelet and granulates is also present as extension of the layer made up of thick granules (indicated by the green arrow).

The layers of granulates can be quite extended, as can be seen in the top left panel of Fig. 5. Their detailed appearance and how they assembly can be appreciated in the subsequent images at growing magnification. At low magnification, the presence of a large mature fiber is also visible.

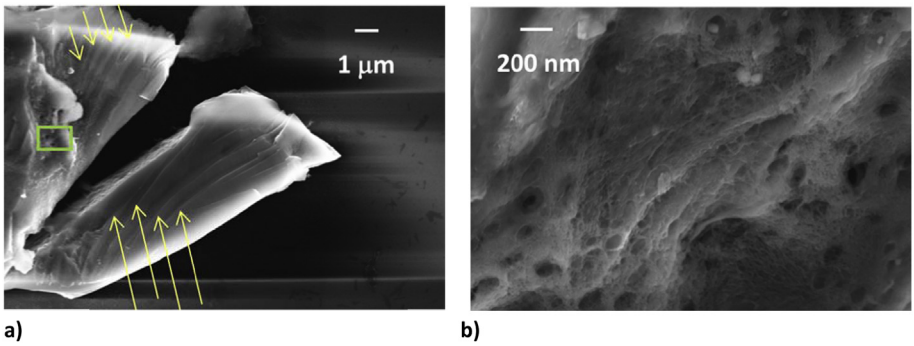

Fig. 3. a) SEM image of the cyt *c* at low concentration (92 μM), aggregated via Tris-HCl below the IP. The yellow arrows indicate the parallel of nearly parallel ripples formed upon aggregation; b) magnification of the area in the green rectangle of panel a).

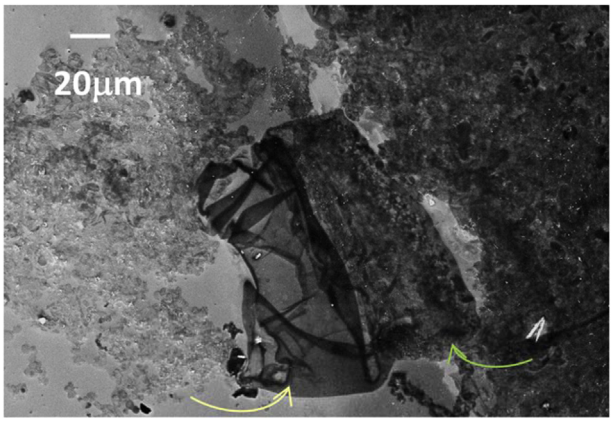

Fig. 4. SEM image of the cyt *c* 100μM, aggregated via NaOH, above the IP, after 1 hour incubation. The yellow arrow indicates an extended platelet, the green one, the extension of the layer made of granules.

The ThT fluorescence image of the sample reveals the presence of diffuse areas with β-sheet character, which include, but are not limited to fibrils (Fig. 5b)).

The loss of the predominant helical secondary structure by incubation of cyt *c* with Tris-HCl below the isoelectric point and with NaOH above the isoelectric point can be appreciated by circular dichroic spectra in the far-UV region. De Groot and Ventura reported that native protein displays two minima at 210 nm and 222 nm, the former shallower than the latter. The conformational changes subsequent to the incubation result in a decrease of the signal strength at 222 nm and a shift of the band at 210 nm towards lower values [4]. In our experimental setup, both effects are observed and they are significantly more pronounced for the incubation with NaOH, in accordance with the whole dataset. This is displayed in Fig. 6 where CD spectra od samples of cyt *c* upon incubation with Tris-HCl for 5 hours and NaOH for ½ hour are reported.

2. Experimental design, materials, and methods

Since the different types of cyt *c* aggregates are achieved by tuning pH and protein concentration in the incubation procedure, the experimental design foresees targeted modulation of the key parameters, by setting the type of base, controlling the exact pH by HCl addition and varying the incubation time. This leads to typical structures/morphologies and structures/morphologies mixtures.

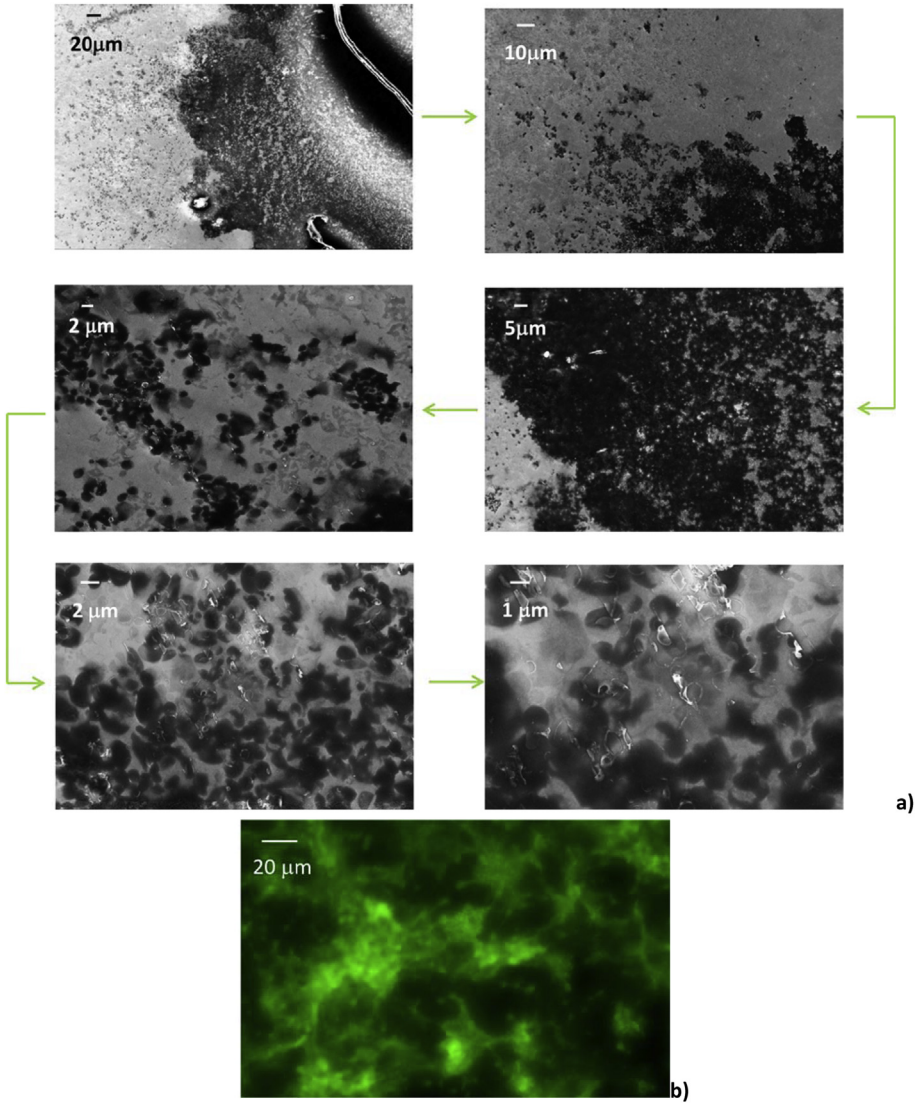

Fig. 5. a) SEM image of the cyt *c* 100μM, aggregated via NaOH, above the IP, after 1 hour incubation, at subsequently larger magnifications (following the green arrows); b) ThT fluorescence image of the same sample.

Lyophilized horse heart cytochrome *c* (C7752) and Thioflavin T (ThT) were purchased by Sigma Aldrich (St. Louis, MO, USA). The protein was dissolved in Tris-HCl buffer (50 mM), or in NaOH (0.1 M). The pH of all solutions was measured with a bench meter instrument (resolution 0.1) and then adjusted to the desired value by small addition of 1 M HCl. Absorption spectra at 408 and 220 nm were acquired prior to imaging experiments in order to measure the exact protein concentration ($e_{408} = 96300$ $M^{-1}cm^{-1}$, $e_{280} = 28500$ $M^{-1}cm^{-1}$). We used a D_2O discharge lamp as light source, coupled with the sample and the monochromator (ACTON RESEARCH mod. 300i) through optical fibers. The optical path within samples was 0.1 cm, the detector a CCD cooled device (1024 × 128 pixel, Toshiba). Data analysis of the spectra was performed with IGOR 6.0 software.

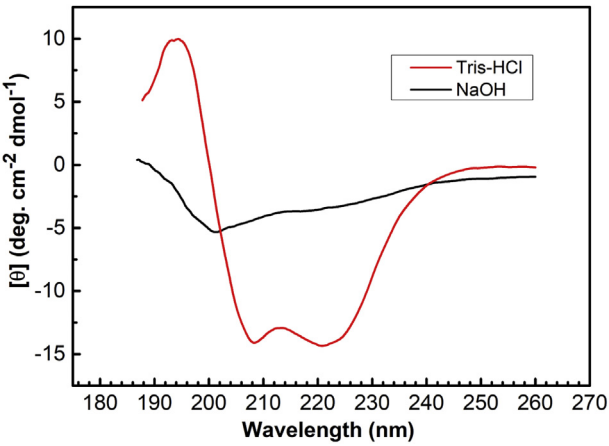

Fig. 6. Far UV-CD spectra of horse heart cyt *c* aggregated via Tris-HCl below the IP for 5 hours (—— red solid line) and via NaOH, well above the IP for ½ hour (—— black solid line).

Solutions were incubated for 8h at 70 °C in a thermal bath. Aliquots of the sample (30 μL for SEM, 10 μL for ThT) were drawn out at regular intervals for SEM and ThT fluorescence imaging.

2.1. SEM imaging procedure

The imaging of the samples may affect by excess of residual base, that causes the presence of bubbles with variable spatial distribution (mainly in the case of Tris-HCl buffer) and the appearance of typical dendritic structures. Therefore, the samples prepared with Tris-HCl were thrice rinsed with deionized water, prior to the deposition on silicon wafers. Samples prepared with NaOH are water soluble, they were first deposited on a silicon wafer and, then, repeatedly (at least thrice) rinsed and dried under inert atmosphere. Control images were acquired along the cleaning processes, until they were cleared from base interference. SEMs images were collected with a Zeiss Auriga Field Emission instrument operating at 7 kV. The images were then processed using Gimp 2.0 open source software package for image treatment.

2.2. ThT fluorescence procedure

For measurement of ThT fluorescence in the presence of amyloid fibrils, 10 μL of sample was stained with 100 μL 0.5% ThT, rinsed with 300 μL of deionized water and finally deposited on microscope slides and dried in-air. Fluorescence images were acquired by a Zeiss optical microscope equipped with a mercury-vapor short-arc-lamp HB = 50 W/AC and 10× objective in the emission spectral range centered at 525 ± 25 nm.

The images were then processed using Fiji open source software package for image treatment and IGOR 6.0 software for particle analysis.

2.3. Circular dichroism

For CD measurements, aliquots of the samples either aggregated via Tris-HCl below the IP and via NaOH above the IP were diluted in distilled water and poured into quartz cuvettes. The CD spectra in the far-UV were collected with a Jasco J-1500 circular dichroism spectrophotometer, equipped with a thermostated cell holder set at 298 ± 0.5 K and purged with ultra-pure nitrogen gas. The ascii files were, then, plotted with the graphical program Origin 9.0.

Conflict of Interest

The authors declare that they have no known competing financial interests or personal relationships that could have appeared to influence the work reported in this paper.

Acknowledgements

Dr. Gabriele Magna and Dr. Donato Monti are gratefully acknowledged for helping out with the collection of the CD data. The research was funded by Progetto Ateneo 2016 and 2017 of Sapienza University of Rome and the MIUR grant carbone_17FFBR.

References

[1] A. Nucara, M. Carbone, F. Ripanti, R. Manganiello, P. Postorino, M. Carbonaro, Achieving cytochrome c fibril/aggregate control towards micro-platelets and micro-fibers by tuning pH and protein concentration: a combined morphological and spectroscopic analysis, Int. J. Biol. Macromol. 138 (2019) 106–115.
[2] M.R.H. Krebs, G. Devlin, A.M. Donald, Protein particulates: another generic form of protein aggregation? Biophys. J. 92 (2007) 1336–1342.
[3] M.R.H. Krebs, K.R. Domike, A.M. Donald, Protein aggregation: more than just fibrils, Biochem. Trans. 37 (2009) 682–686.
[4] N.S. de Groot, S. Ventura, Amyloid fibril formation by bovine cytochrome c, Spectroscopy 19 (2005) 199–205.